Chitosan-coated mesoporous silica nanoparticles for suppression of *Fusarium virguliforme* in soybeans (*Glycine max*)

Tana L. O'Keefe, ^{1†} Chaoyi Deng, ^{2†} Yi Wang, ² Sharmaka Mohamud, ¹ Andres Torres-Gómez, ² Beza S. Tuga, ^{1‡} Cheng-Hsin Huang, ^{1‡} Wilanyi R. Alvarez Reyes, ^{1‡} Jason C. White, ² Christy L. Haynes ^{1*}

KEYWORDS: silica nanoparticles, chitosan, soybeans, disease suppression, biotic stress

ABSTRACT

There is a need to develop new and sustainable agricultural technologies to help provide global food security, and nanoscale materials are showing promising results in this area. In this study, mesoporous silica nanoparticles (MSNs) and chitosan-coated mesoporous silica nanoparticles (CTS-MSNs) were synthesized and applied to soybeans (*Glycine max*) by two different strategies in greenhouse and field studies to study the role of dissolved silicic acid and chitosan in enhancing plant growth and suppressing disease damage caused by *Fusarium virguliforme*. Plant growth and health were assessed by measuring soybean biomass and chlorophyll content in both healthy and *Fusarium*-infected plants at harvest. In the greenhouse study, foliar and seed applications with 250 mg/L nanoparticle treatments were compared. A single seed treatment of MSNs reduced disease severity by 30% and increased chlorophyll content in both healthy and infected plants by 12%. Based on greenhouse results, seed application was used in the follow-up field study, and MSNs and CTS-MSNs reduced disease progression by 12% and 15%, respectively. A significant 32% increase was observed for chlorophyll content for plants treated with CTS-MSNs. Perhaps most important, nanoscale silica seed treatment significantly increased (23-68%) the micronutrient (Zn, Mn, Mg, K, B) content of soybean pods, suggesting a potential sustainable strategy for nano-

¹ Department of Chemistry, University of Minnesota, 207 Pleasant Street SE, Minneapolis, MN 55455, United States

² Connecticut Agricultural Experiment Station, 123 Huntington Street, New Haven, CT 06511, United States

enabled biofortification to address nutrition insecurity. Overall, these findings indicate that MSN and CTS-MSN seed treatments in soybeans can enable disease suppression and increased plant health as part of a nano-enabled strategy for sustainable agriculture.

INTRODUCTION

The global population is expected to exceed 9.7 billion by 2050, and current estimates predict that global food production must increase substantially to achieve and maintain global food security. As part of the United Nation's Zero Hunger goal, there are hopes to ensure sustainable food production systems and implement resilient agricultural practices to increase productivity and production by 2030. In addition to needing more food for the growing global population, more nutritious food is also needed as more than 2 billion people have critical micronutrient deficiencies that lead to poor health outcomes that could be prevented. As an economically important crop, with over 372 million tons being produced globally in 2021,² soybeans can play a crucial role in providing food security and helping to meet the Zero Hunger goal. However, plant diseases pose a huge threat to agriculture, with anywhere from 20-40% of crops being lost to pathogens each year.³ Fusarium diseases are significant hindrances to food plant production as there are at least 20 different species that infest more than two dozen crop species.⁴ Specifically, Fusarium virguliforme (FV) is a soil-borne fungal pathogen that causes sudden death syndrome (SDS) to soybeans (Glycine max). When infected with FV, phytotoxins move from roots to shoots within the plant's vascular system, causing SDS and resulting in tissue damage and discoloration to foliar tissues.^{5,6} SDS is widespread in the United States and has resulted in \$6.75 billion dollars in losses from 1996 to 2016, with annual yield losses ranging from 0.6 to 1.9 million metric tons from 2006 to 2014.^{7, 8} The protection of crops from plant diseases plays an obvious and important role in meeting the growing global demand for food; ideally, this would be done without increased application of pesticides or soil fumigation. Management of SDS has been challenging, although techniques such as fungicide seed treatments,^{9, 10} breeding and selection of cultivars with hostplant resistance,^{11, 12} improving soil drainage,¹³ and crop rotation¹⁴ have had limited success. However, none of these management options have performed well across a range of environmental conditions that plants may experience in the field. Thus, there is a pressing need for sustainable agricultural techniques to manage these pathogens.

Previously, nanoparticles (NPs) have proved to be an effective treatment for *Fusarium* strains in other plants species such as watermelon (Citrullus lanatus), 15-17 tomatoes (Solanum lycopersicum), ^{18, 19} and lettuce (Lactuca sativa)²⁰ due to the small size that allows for enhanced plant uptake and distribution. Silica NPs are a sustainable option for use in agriculture as silicon is the second most abundant element in the Earth's crust. Furthermore, silicon, while not an essential nutrient for plants, can enhance plant health and growth and has been found to alleviate many abiotic and biotic stresses within plants. 21, 22 Silicon is usually acquired through a plant's roots as silicic acid, where it can then form a cuticle-silica double layer barrier that fortifies the plant's cell wall to facilitate protection against disease.²¹ Additionally, silicon activates plant defense mechanisms through the production of stress hormones, such as phytoalexins, or through the synthesis of antimicrobial compounds within the plant.²³ Silica NPs are known to dissolve to release silicic acid, and Kang et al. has shown that the dissolution rate correlates with the suppression of Fusarium wilt, with faster dissolution increasing crop health and fruit yield in watermelon (C. lanatus).¹⁷ Furthermore, mesoporous silica nanoparticles (MSNs) have high surface areas and pore volumes that make them particularly useful for agrochemical delivery; this has been demonstrated in tomatoes (S. lycopersicum),²⁴ cucumber (Cucumis sativa),²⁵ wheat (Triticum aestivum), 26 and soybeans (G. max). 27

Chitosan, an organic polysaccharide, has also been shown to increase disease resistance by initiating a signaling cascade within plants to increase their natural defense mechanisms. ^{28, 29} In addition to the enhancement of natural defense mechanisms, chitosan has been reported to have antifungal properties that may provide protection against pathogens. ^{30, 31} Furthermore, chitosan is naturally derived from chitin, making it a sustainable material for use in agriculture. For these reasons, chitosan NPs have been applied in agricultural applications with demonstrated disease suppression in tomatoes (*S. lycopersicum*)³² and chickpeas (*Cicer arietrium*). ³³ Since silica NPs and chitosan act through two different mechanisms to alleviate plant disease, these two materials have been combined to further enhance disease suppression. ^{34, 35} Although previous work with CTS-MSNs showed suppression of *Fusarium* wilt and enhanced plant growth in species known to accumulate Si, such as watermelon, ¹⁵ much remains unknown about other plant species, including soybeans, that are low Si accumulators.

Therefore, in this work, mesoporous silica nanoparticles (MSNs) and chitosan-coated mesoporous silica nanoparticles (CTS-MSNs) were applied to soybeans (*Glycine max*) to assess their impact on indicators of plant health. MSNs were synthesized and coated with chitosan under acidic conditions to produce CTS-MSNs. Both MSNs and CTS-MSNs were characterized with dynamic light scattering (DLS), ζ -potential measurements, transmission electron microscopy (TEM), and nitrogen physisorption, in addition to a silicomolybdic acid (SMA) spectrophotometric assay to assess their dissolution behavior prior to plant application. A novel vacuum infiltration technique was used to infiltrate MSNs and CTS-MSNs into soybean seeds, and this exposure route was compared to the traditional foliar application in a greenhouse study. Plant growth, biomass, and chlorophyll content were assessed in healthy and *Fusarium*-infected plants. The silicon content in plant shoots, roots, and soybean pods was determined with inductively coupled plasma-optical

emission spectroscopy (ICP-OES). The greenhouse findings revealed the effectiveness of an MSN seed treatment in enhancing plant growth and reducing disease progression; thus, a seed treatment was advanced to a field study where CTS-MSNs showed higher disease suppression, suggesting that CTS-MSNs may have more of a long-term impact on soybeans. In the field, nanosilica treatment also significantly increased the micronutrient content of soybean pods. Together, these studies show the positive impact of combining mesoporous silica nanoparticles with chitosan on an economically important crop, soybeans, in the field, offering great potential as a sustainable solution for nano-enabled agriculture.

EXPERIMENTAL SECTION

Materials. Cetyltrimethylammonium bromide (CTAB), tetraethyl orthosilicate (TEOS), chlorotrimethylsilane (TMS), chitosan (50-190 kDa), ammonium molybdate tetrahydrate, oxalic acid, 4-methylaminophenol sulfate, sodium sulfite (anhydrous), concentrated hydrochloric acid (37%), and silicon standard solution (1000 ppm) were obtained from Sigma-Aldrich (St. Louis, MO). Ammonia nitrate (NH4NO3), citric acid, malic acid, and concentrated sulfuric acid (95-98%) were obtained from Fisher Chemical (Ottawa, ON). Malic acid was obtained from Acros Organics (Geel, Belgium). 2-[methoxy(polyethyleneoxy)9-12propyl]-trimethoxysilane, tech-90 was obtained from Gelest, Inc. (Morrisville, PA). Ammonium hydroxide (NH4OH, 28-30% as NH3), glacial acetic acid, and sodium hydroxide were purchased from Avantor (Radnor, PA). Absolute ethanol was acquired from Decon Labs, Inc. (King of Prussia, PA). Ultrapure water was purified using a Milli-Q Millipore water purification system (Billerica, MA)

Synthesis of MSNs. MSNs were synthesized using a previously reported method with modifications.³⁶ Briefly, 0.29 g of CTAB was mixed with 150 g of 0.256 M NH₄OH in an Erlenmeyer flask and was covered and stirred for 1 h at 500 rpm and 50 °C. After 1 h, 2.5 mL of

0.88 M TEOS in ethanol was added dropwise via addition funnel. This solution was stirred for 1 h at 700 rpm and 50 °C to form the silica framework around the CTAB micelles. Next, 450 μ L 2-[methoxy-(polyethyleneoxy)₉₋₁₂propyl]-trimethoxysilane was slowly added to the solution and stirred for 30 min at 700 rpm and 50 °C. Then, 68 μ L of TMS was added and stirred for 30 min at 700 rpm and 50 °C. After the 30 min, the solution was aged in a beaker at 50 °C for 20 h. The MSNs were purified using ultracentrifugation at $61,579 \times g$, under vacuum, for 30 min. The supernatant was removed, and the pellet was re-dispersed in 6 g/L ethanolic NH₄NO₃ to perform an ion exchange reaction to remove the CTAB micelles. The suspension was stirred under reflux for 1 h at 50 °C before ultracentrifuging and washing with 190 proof ethanol. Another reflux step using 6 g/L ethanolic NH₄NO₃ was carried out with three more washes with increasing ethanol concentrations (95%, 99%, and 99% ethanol in water). The final suspension was dried using rotary evaporation to collect the dried MSNs.

Chitosan Coating of MSNs. A procedure from Chen et al. was adapted for coating the MSNs with chitosan.³⁷ Briefly, a 0.6% w/v solution of chitosan was prepared in 10% v/v acetic acid in water. The pH of the solution was adjusted to 5.5 with 1 M NaOH and then dried MSNs were added to the chitosan solution to prepare a 0.5% w/v suspension (typically with 100 mg of MSNs added to 20 mL of chitosan solution). The suspension was then stirred at room temperature for 48 h to allow for the formation of hydrogen bonds between the silanol groups on the surface of the MSNs and the amine groups on chitosan. Excess chitosan was removed by centrifugation at 17,000 x g for 15 min. Chitosan-coated MSNs (CTS-MSNs) were then resuspended in Milli-Q water and dried using a rotary evaporator.

Transmission Electron Microscopy (TEM). To prepare the MSNs for TEM, the nanoparticles were suspended in ethanol at 0.5-1 mg/mL and sonicated for 15 min to ensure adequate dispersion.

Then, 200 mesh copper grids with Formvar and carbon supports (Ted Pella, Inc., Redding, CA) were dipped into the suspension and dried in an oven at 50 °C for 5 min. For CTS-MSNs, the nanoparticles were suspended in Milli-Q water at 0.5 mg/mL. TEM grids were dipped in solution and dried as described above. TEM images were acquired by random sampling of grid sections using a FEI Tecnai Spirit Bio-Twin transmission electron microscope using a 120 kV operating voltage.

Dynamic Light Scattering and ζ**-Potential Measurements.** After the synthesis of MSNs and coating CTS-MSNs, the nanoparticles were resuspended in water at 0.5-1 mg/mL. The suspensions were sonicated for 15 minutes prior to characterization to ensure adequate dispersion. The hydrodynamic diameters and ζ-potentials were then determined for three material replicates using a Malvern Zetasizer Pro instrument (Westborough, MA).

Nitrogen Physisorption. Nitrogen physisorption was performed to determine the surface area and pore volume of the MSNs and CTS-MSNs. Approximately 60 mg of MSNs or CTS-MSNs were added to the sample glassware. The samples were degassed prior to analysis at cryogenic temperatures on a Micromeritics ASAP 2020 instrument (Norcross, GA). The surface area and pore volume were determined using the Brunauer-Emmett-Teller (BET) and Barrett-Joyner-Halenda (BJH) methods, respectively.

Silicomolybdic Acid (SMA) Spectrophotometric Assay. Two solutions were prepared for the silicomolybdic acid assay that has been previously reported.³⁸ Solution A was prepared by mixing 30 mL of concentrated hydrochloric acid into 400 mL of Milli-Q water in a 500 mL volumetric flask. Next, 10 g of ammonium molybdate tetrahydrate was added and the solution was diluted to 500 mL with Milli-Q water. Solution B was prepared by mixing 100 mL of concentrated sulfuric acid into 800 mL of Milli-Q water in a 1L volumetric flask. Then, 20 g of oxalic acid, 6.67 g of 4-

methylaminophenol sulfate, and 4 g of anhydrous sodium sulfite were added. The solution was diluted to 1 L with Milli-Q water. The assay was performed in simulated xylem sap which consisted of 1.71 mM citric acid and 890 M malic acid in Milli-Q water with an adjusted pH of 6.0.\(^{16}\) For the assay, each nanoparticle was dispersed in simulated xylem sap at 250 mg/L and sonicated to ensure adequate dispersion. The suspensions were incubated at ambient temperature for the duration of the experiment (50 days). At each timepoint, 0.5 μ L of the suspension was removed and diluted with 800 μ L of Milli-Q water in a 48-well plate. Then, 75 μ L of solution A was added and incubated for 10 minutes at ambient temperature. Next, 375 μ L of solution B was added. The plate was incubated at ambient temperature for 2 h. Optical density measurements at 810 nm were recorded on a Biotek Synergy H1 microplate reader (Winooski, VT) to quantify reduced silicomolybdic acid, also known as the molybdenum blue complex. The silicic acid concentration was calculated by comparison of the optical densities of the sample mixtures to those of the diluted silicon standard solutions.

Seed Germination and Transplanting. For the greenhouse experiment, plastic pots measuring 12.5 cm in diameter and 10 cm in height underwent cleaning with Milli-Q water before being filled with 0.5 L of commercial potting mix soil (Pro-Mix BX, Premier Hort Tech, Quakertown, PA) purchased from a local market in New Haven, CT. The potting soil contained a Si content of 30.2 \pm 0.5 mg/kg. The germination of soybean seeds occurred in a starter germination kit, and after a 15-day period, the seedlings were transplanted individually into each pot. Post-sowing, the seedlings and ensuing plants were cultivated in a greenhouse maintaining a temperature range of 25 \pm 5 °C. Regular watering was administered to sustain soil moisture at approximately 60% of its field capacity, occurring every two days, without any additional fertilizer application. The arrangement of the pots followed a completely randomized design.

For the field experiment, the experimental site was established at the Connecticut Agricultural Experiment Station's Lockwood Farm located in Hamden, Connecticut. The soil was previously characterized as a Cheshire Fine Sandy Loam with a pH of 5.9.39 Microplots were established in spring 2023 with rows 0.9 m wide and spaced 6 m apart. The plots were fertilized with 112 kg/ha of 10-10-10 NPK, covered with black plastic mulch, and irrigated using drip tape. Thirty microplots were created within the rows, each separated by 30 cm. Seedlings grew for four weeks in plastic liners (36-cell, 5.66 ×5.66 ×4.93 cm³) with potting soil substrate before transplanting. No fertilizer was applied during this period. Uniform, four-week-old seedlings were selected as transplants for the field study. In Fusarium-infested microplots, planting holes were hand-mixed with 0.75 g of millet inoculum (see below) just before transplanting. For non-infested plots in adjacent rows, the same preparation method was used, but no pathogen was introduced. **Preparation of Millet Inoculum.** The pathogen inoculum was prepared according to previous reports.⁴⁰ Briefly, millet (Echinochloa esculenta) seeds were autoclaved in distilled water (1:1, wt:wt) for 1 h seeded with two agar plugs colonized with Fusarium virguliforme (FV). After incubating at 22-25 °C for three weeks, the millet was air-dried, ground, sieved to 1 mm, and added to the soil.

Nanoparticle Application. In this study, we employed two methods of Si-based nanoparticle amendment to soybean plants: seed infiltration and foliar spray. By comparing these methods, we aimed to discern the most effective approach for introducing Si-based materials into the plants. For seed infiltration, the seeds were treated separately with CTS-MSN, MSN, chitosan control, or silicic acid control suspension/solution to achieve final Si concentrations of 250 mg/kg (except for the chitosan control), aligning with levels used in field soils in prior research. Following immersion in the suspension/solution, the seeds underwent a 30-minute vacuum infiltration to

remove air, followed by a 30-minute rest to facilitate penetration of the suspension/solution. The control treatment involved the addition of only Milli-Q water. Regarding the foliar spray method, suspensions/solutions were loaded into different commercial spray bottles and sonicated before application. A surfactant was added to the solution to minimize aggregation and maximize particle retention on the plant leaf surface. The plants received 5 mL of suspension every two days for a total of three applications (15 mL overall), with the initial spray administered five days post-transplanting. This yielded a total of 3.75 mg (250 mg/L) of silica per plant, mirroring the seed treatment. To prevent contamination, the soil surface was covered with plastic film prior to application. Ten replicates were established for each treatment for both application methods.

Plant Harvest. Plants were rated weekly for disease progression based on plant shoot system phenotype, and the area-under-the-disease-progress curve (AUDPC) was calculated using Eq. 1 shown below.⁴¹ Disease severity was determined based on a scale of 1–5, where 1 = healthy, 2 = slightly stunted, 3 = partially stunted, 4 = severely stunted, 5 = completely stunted or dead. AUDPC calculations were made using the trapezoid rule:

AUDPC=
$$[D_i+D_{(i+1)}]/2 \times (t_{(i+1)}-t_i)$$
 (Eq. 1)

where D_i =the disease rating at time t_i. Sixty days post-transplanting, plants were harvested. Root, shoot, and pod samples were collected and underwent three thorough cleanings with Milli-Q water to eliminate soil and nanoparticles adhered to their surfaces before subsequent analysis. Prior to harvesting, the average chlorophyll content of five randomly chosen leaves from each plant was measured using a handheld single-photon avalanche diode chlorophyll meter (SPAD, Minolta Camera, Japan). Following harvest, fresh samples were weighed and oven-dried at 70 °C for three days for subsequent analysis.

Nutrient Analysis. For the assessment of elemental content in tissues, dry samples were ground in a mortar, and 0.2 g was precisely weighed into 50 mL digestion tubes. Subsequently, 5 mL of trace pure nitric acid was added to each sample. The samples underwent digestion in a digiPrep hot block (SCP Science, Quebec, Canada) for 45 minutes at 115 °C. Following digestion, the tubes were brought to a 50 mL volume with Milli-Q water. The Si concentration, along with selected macro and micro elements, was determined using an inductively coupled plasma-optical emission spectrometer (ICP-OES, Perkin-Elmer Optima 4300 DV; Shelton, CT). To ensure quality control, a blank sample and a NP-spiked sample of known content were analyzed every 30 samples. Additionally, a standard reference material (NIST 2709a, Gaithersburg, MD) was included. Statistical Analysis. For comparisons for the characterization of MSNs and CTS-MSNs, paired ttests were used to determine statistical significance. Values reported for the MSN and CTS-MSN characterization are denoted as mean \pm standard deviation. For plant exposures, statistical analysis was performed separately for foliar and seed application and on healthy and Fusarium-infected plants using a one-way ANOVA with Dunnett's multiple comparisons test (p < 0.05) unless otherwise noted. For the greenhouse and field study, five and six replicates were included, respectively. For plant-based endpoint measurements (pigment and element content), six replciates were used.

RESULTS AND DISCUSSION

Characterization of MSNs and CTS-MSNs. TEM was used to analyze the structure of the MSNs and chitosan-coated MSNs (Figure 1a,b). Both particles are spherical in shape as expected. The TEM images for MSNs show clear mesopores that are obstructed upon the addition of a chitosan coating, indicating the coating was successful. The effective hydrodynamic diameters and ζ -potentials were measured before and after chitosan coating and also confirm the presence of the

coating (Figure 1c,d). The hydrodynamic diameter of MSNs is approximately 117 \pm 19 nm. Upon coating MSNs with chitosan, the hydrodynamic diameter more than triples (385 \pm 92 nm), suggesting some slight aggregation of the CTS-MSNs. For MSNs, the ζ -potential is -35 \pm 3 mV while CTS-MSNs have a slightly less negative ζ -potential of -25 \pm 2 mV that is statistically significant. The observed shift in ζ -potential upon applying a chitosan coating is attributed to the positively charged polysaccharide binding with and blocking the silanol groups on the MSNs surface. The negative ζ -potential of CTS-MSNs contradicts previous reports of chitosan-coated silica NPs. This is potentially due to the aggregation and instability of the CTS-MSNs, resulting

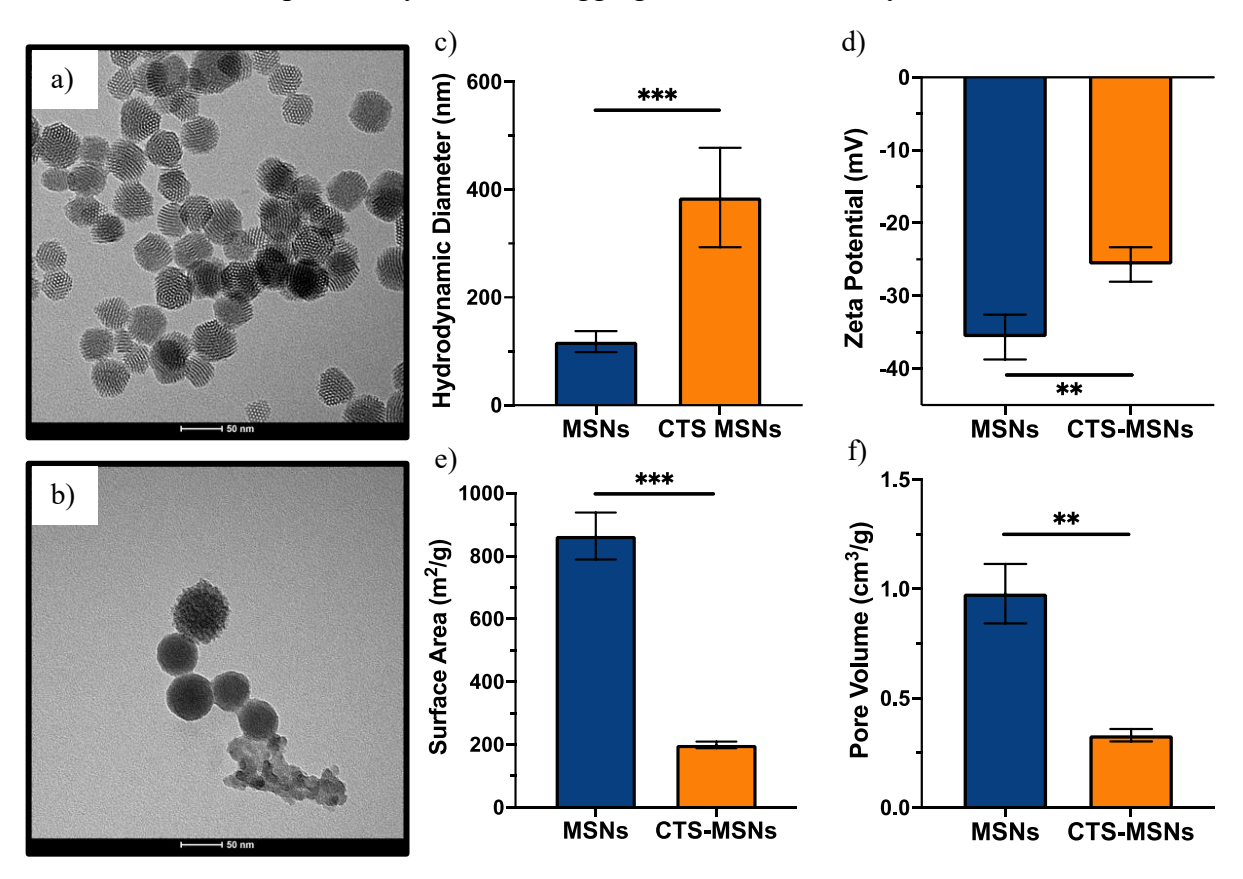


Figure 1. Representative TEM images of a) MSNs and b) CTS-MSNs. Physical characteristics of bare MSNs and CTS-MSNs after performing the chitosan coating with a (c) hydrodynamic diameter increase upon coating and (d) a less negative ζ -potential observed for CTS-MSNs. A (e) decrease in the surface area that indicates blocked pores in the CTS-MSNs, and (f) a decrease in pore volume, again indicating blockage of the pores by chitosan. Error bars represent the standard deviation of triplicate measurements. Paired t-tests were used to determine statistical significance. **p < 0.01, ***p < 0.001

in a ζ -potential measurement that is representative of the colloidally stable CTS-MSNs that remain in solution. Nitrogen physisorption was performed to assess the surface area and pore volume change after applying the chitosan coating (Figure 1e,f). A decrease in both surface area and pore volume supports that chitosan is coating or blocking the MSN pores, decreasing the effective internal surface area of the MSNs, as well as their overall pore volume. Thermogravimetric analysis was performed to determine the mass contribution of chitosan in the CTS-MSNs (Figure S1). Based on three material replicates of CTS-MSNs, approximately $20 \pm 2\%$ of the CTS-MSN mass was from the chitosan coating, which agrees with previously reported thermograms and ranges of chitosan coating on MSNs. 15, 42 To keep the concentration of silica consistent across MSN and CTS-MSN treatments in the greenhouse and field studies, the applied concentration of CTS-MSNs was increased by 20%.

Dissolution Rates of MSNs and CTS-MSNs. Since silicic acid, a dissolution product of silica NPs in water, is the critical species for plant assimilation, the dissolution rates of both NP types

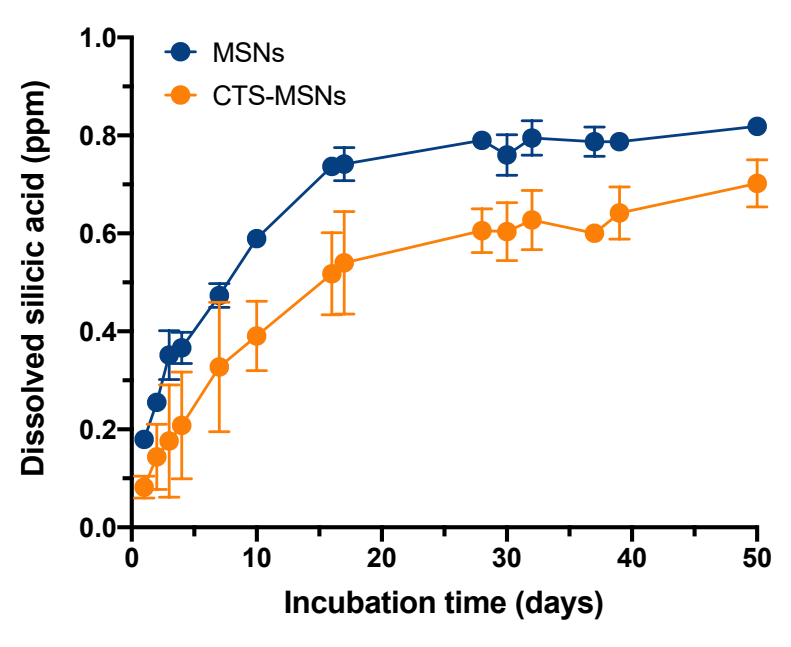


Figure 2. Silicomolybdic acid spectrophotometric assay results for three material replicates of MSNs (blue) and CTS-MSNs (orange) in simulated xylem sap. Error bars represent the standard deviation at each measurement time point; when error bars are not visible, they are smaller than the symbol used to represent the average value.

were assessed ahead of greenhouse and field studies. A silicomolybdic acid spectrophotometric assay was performed to quantify the monomeric or oligomeric silicic acids released from the MSNs and CTS-MSNs. Simulated xylem sap was used as a model of natural vascular media, which is an interior fluid of plants responsible for root-to-shoot nutrient and water transport. The dissolution was assessed over 50 days, which is approximately the length of the greenhouse and field study and also when the measured silicic acid plateaued. Over the course of 50 days, 250 mg/L of MSNs released 0.82 ± 0.1 ppm of silicic acid, which was statistically greater than the 0.70 ± 0.05 ppm of silicic acid released from CTS-MSNs. The MSNs released more silicic acid than CTS-MSNs, and the release was more rapid than the coated particles. The slower dissolution and smaller concentration of silicic acid released with chitosan coating is likely due to restricted water access to the particle's surface, slowing hydrolysis and dissolution of the CTS-MSNs. Previously, published literature has shown that concentrations of silica nanoparticles ranging from 25-1600 ppm have been beneficial for plant growth and disease suppression. 17, 43, 44 While the concentration of released silicic acid from MSNs and CTS-MSNs is low, Si is not an essential nutrient for plants. Rather, it is considered a beneficial element and concentrations of silicic acid as low as 1 ppm could enhance a plant's defense mechanisms against disease; this is based on reports demonstrating that 1-3 ppm of micronutrients such as Zn, Cu, and B could enhance a plant's natural defenses. 45-47

Greenhouse and Field Study. Both a greenhouse experiment and field study were carried out to study the impact of MSNs and CTS-MSNs on healthy and *Fusarium*-infected soybeans (Figure 3). In the greenhouse study, seed and foliar amendments were applied to soybeans growing in both healthy and infected soil to investigate differences in the application method of the MSNs and CTS-MSNs. Based on greenhouse results, the seed application was selected for the field study. It should be noted that the materials cost associated with foliar or seed application is approximately \$0.02 per seedling, 15 making these materials a cost effective treatment.

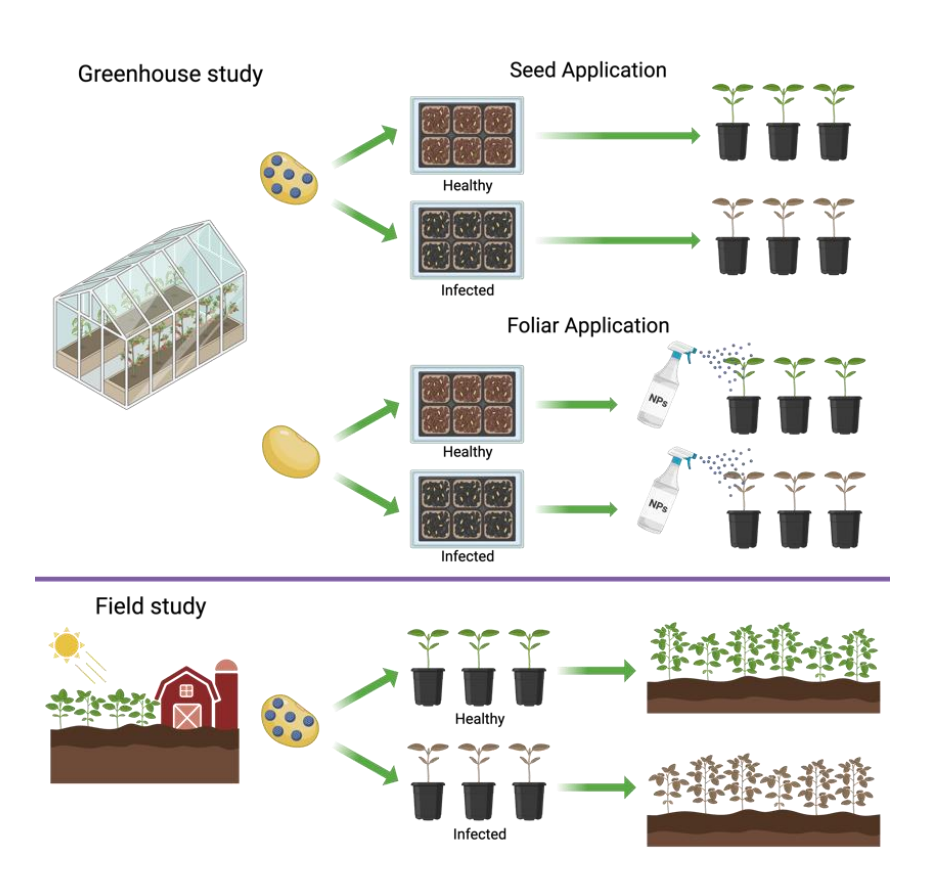


Figure 3. Experimental scheme for the greenhouse and field studies.

Role in Disease Suppression. In the greenhouse experiment, the impact of foliar and seed applications of MSNs and CTS-MSNs on suppressing *Fusarium* wilt was evaluated using the AUDPC (Figure 4a). For infected plants, there was no change in the AUDPC for soybeans receiving the foliar application, although there is a non-significant trend that the two NP treatments performed better, with nominally lower AUDPC values. However, for seed treatments, MSN treatment resulted in a statistically significant \sim 30% decrease in disease presence. This reduction is likely due to a statistically significant increase in the Si concentration (68 \pm 9 ppm) that is incorporated into the soybean seed upon MSN treatment (Figure S2) when compared to the untreated control (19 \pm 9 ppm), which is also non-significantly greater than the Si content from the CTS-MSN treatment (58 \pm 6 ppm). Additionally, the CTS-MSNs appeared to outperform the

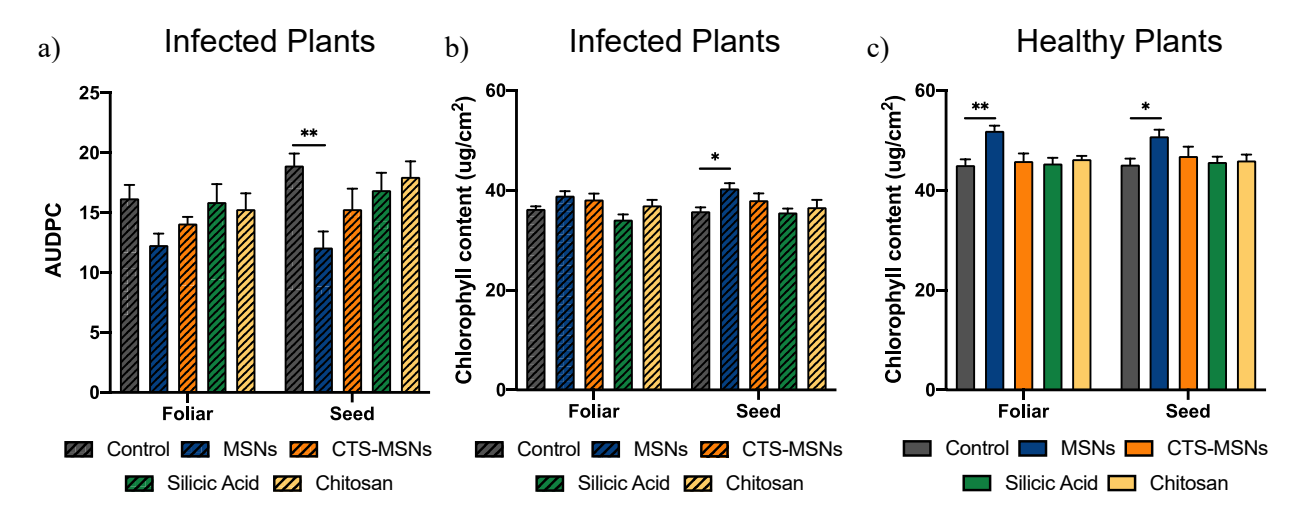


Figure 4. a) Area under the disease progress curve (AUDPC) for *Fusarium*-infected plants that received foliar application (left side) and seed infiltration (right side) of different forms of Si and/or chitosan. Chlorophyll content for foliar and seed treatments in (b) *Fusarium*-infected plants and (c) healthy plants for the greenhouse study. The error bars represent the standard error of five replicate plants. A one-way ANOVA with Dunnett's multiple comparisons was used to evaluate the statistical significance for foliar and seed applications separately. Graphs for foliar and seed application are shown together for ease of comparison. *p < 0.05, **p < 0.01

conventional bulk treatment, although the difference was not of statistical significance. The reduced response of CTS-MSNs and the lack of response from chitosan indicates that silica plays

a larger role in bolstering the soybean defenses against *Fusarium*, although the larger size and greater potential for aggregation of CTS-MSNs may have also reduced the uptake into the plant. However, the lack of response from chitosan indicates that silica plays a greater role in enhancing soybean defenses against *Fusarium*. Silicic acid also did not suppress *Fusarium* wilt, further highlighting the importance of the nanoscale size and/or extended dissolution for effective disease management.

At harvest, the chlorophyll content of leaves from five plant replicates was measured as another means to assess plant health (Figure 4b,c). Chlorophyll is crucial for the photosynthetic process of plants, and greater amounts of chlorophyl result in an increased potential for photosynthetic outputs, while decreased amounts serve as an indicator for soybean SDS. Additionally, plants with higher chlorophyll content often produce more nutrients, aiding the plant's resistance to environmental stresses, such as fungal infection. In this study, infection alone reduced the chlorophyll content by $\sim 20\%$, decreasing from approximately 45 $\mu g/cm^2$ in healthy controls to 36 µg/cm² for Fusarium-infected controls. In healthy plants, MSNs significantly increased the chlorophyll content for both foliar and seed application (~15% and ~12%, respectively), suggesting an increase in overall plant health and that nanoparticle treatments would be beneficial even to healthy plants. Additionally, in infected plants, chlorophyll content was significantly increased by ~12% in plants that received the seed treatment of MSNs, almost completely alleviating the decrease induced by disease. This is supported by literature where increases in chlorophyll content have previously been correlated to overall plant health upon silica nanoparticle treatments.^{48, 49}

Changes in Biomass after NP Treatment. The fresh biomass was also measured for healthy and diseased plants that were treated with foliar or seed applications of MSNs and CTS-MSNs, as well

as untreated controls (Figure 5). Disease had no impact on the biomass of shoots, roots, and pods when comparing the control groups for healthy and Fusarium-infected plants; this indicates that the disease pressure was low in the greenhouse study. For healthy soybeans that were seed treated, there is a statistically different increase in the shoot masses for all treatments with a 61% increase for MSNs and a 55% increase for CTS-MSNs. Although there are no statistically significant differences, there is a clear trend of MSNs and CTS-MSNs increasing biomasses for shoots, roots, and soybean pods for both foliar and seed applications. In infected soybeans, there are no changes or clear trends for nanoscale or bulk treatments applied foliarly. Conversely, MSN and CTS-MSN seed treatments resulted in greater biomasses for the infected soybeans with statistically significant increases for CTS-MSNs and MSNs in the roots and soybean pods, respectively. As the soybeans germinate, it is expected that the roots are the first to experience the seed treatment of MSNs and CTS-MSNs, resulting in thicker plant cell walls, greater initial protection, and subsequently higher biomasses. The different tissue biomass responses of plants to treatment as a function of disease status is notable and is likely due to the underlying shift in plant physiology and biochemistry as a function of infection. This is further supported by trends in the tissue element data as determined by IPC-OES (Figure S3 and S4) where higher Si concentrations are observed in the roots of soybeans treated with MSNs and CTS-MSNs. Overall, MSNs and CTS-MSNs improved soybean growth in the presence and absence of Fusarium, with more differences observed with seed treatments. Based on the impact of seed treatments with MSNs and CTS-MSNs as determined by AUDPC, chlorophyll content, and biomass results, the field study was carried out using this treatment strategy.

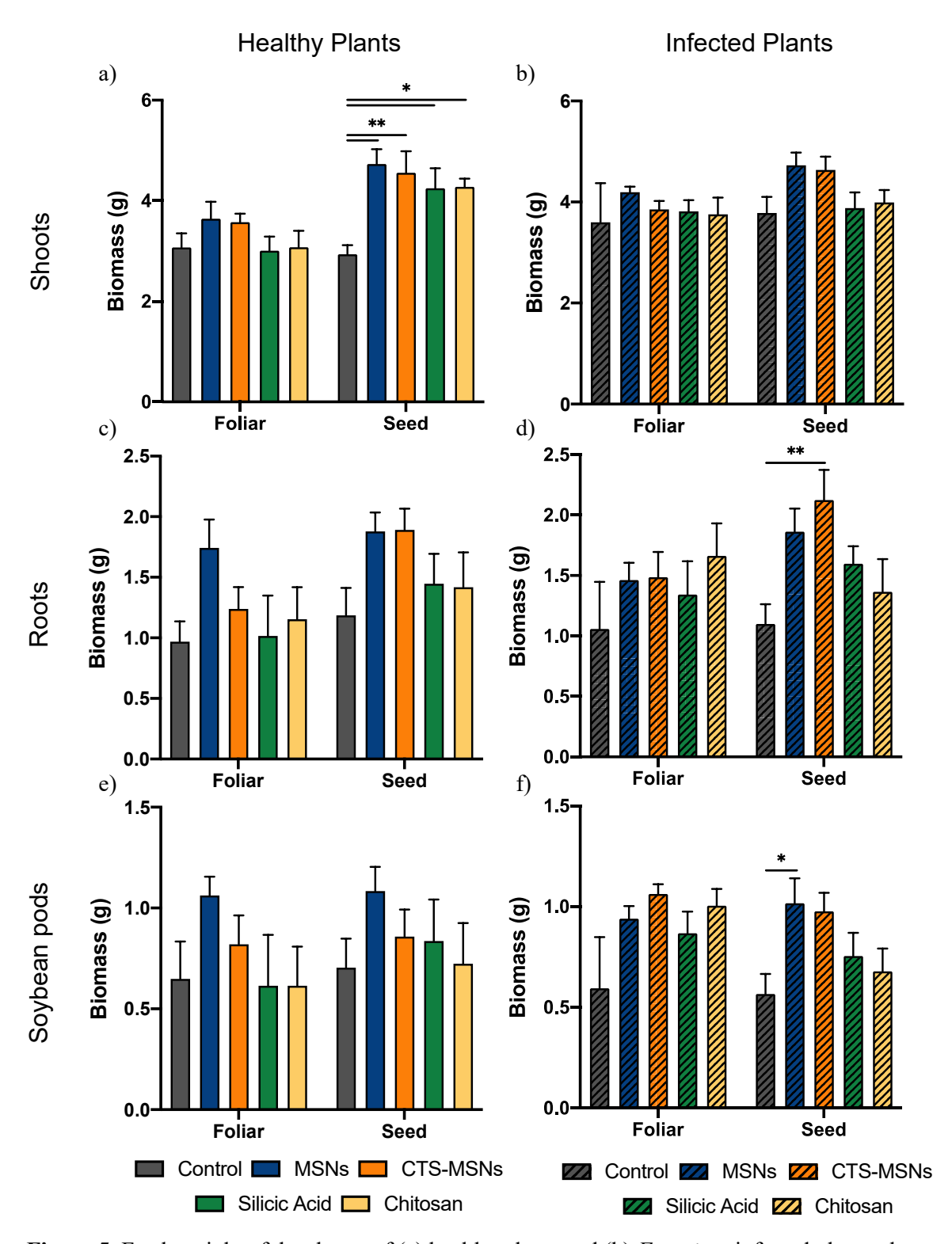


Figure 5. Fresh weight of the shoots of (a) healthy plants and (b) *Fusarium*-infected plants; the roots of (c) healthy plants and (d) *Fusarium*-infected plants; the soybean pods of (e) healthy plants and (f) *Fusarium*-infected plants from the greenhouse study. The error bars represent the standard error of five replicate plants. A one-way ANOVA with Dunnett's multiple comparisons was used to evaluate statistical significance for foliar and seed applications separately. Graphs for foliar and seed application are shown together for ease of comparison. *p < 0.05, **p < 0.01

Field Study. AUDPC was also used in the field study to monitor the rate and level of disease damage (Figure 6a). Although there were no statistically significant changes in the AUDPC across treatments, there was a clear trend of MSNs and CTS-MSNs suppressing infection (~12-15% AUDPC reduction) in comparison to the control, as well as the silicic acid and chitosan treatments. The lack of significant changes upon treatment may be due to the complexity of field studies, as well as the fact that overall disease pressure in this study appears to have been low. However, it should be noted that this trend with the two NP treatments reducing the AUDPC agrees with the greenhouse study.

Leaf chlorophyll content was measured at harvest; overall, disease reduced chlorophyll content by ~20% with pigment content decreasing from approximately 48 μ g/cm² in the healthy control to 38 μ g/cm² for the infected controls. There were no changes in chlorophyll content as a function of treatment for the healthy plants (Figure 6b). Conversely, for infected plants, a significant increase (~32%) in chlorophyll levels was observed for CTS-MSN-treated plants (Figure 6c), effectively returning the chlorophyll levels to that of the healthy control. This increase

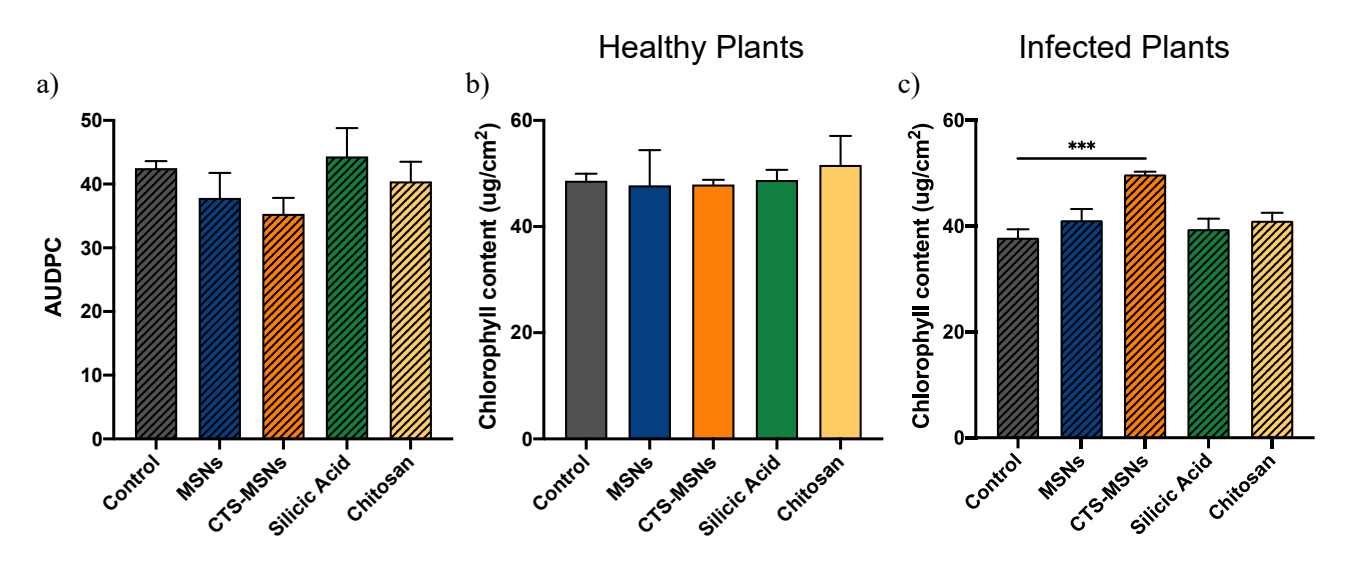


Figure 6. (a) AUDPC for *Fusarium*-infected plants. Chlorophyll content for (b) healthy plants and (c) *Fusarium*-infected plants. The error bars represent the standard error of five replicate plants. A one-way ANOVA with Dunnett's multiple comparisons was used to evaluate statistical significance. ***p < 0.001

in chlorophyll aligns well with the 15% reduction in AUDPC for CTS-MSNs, clearly demonstrating that this treatment resulted in healthier plants. Notably, in the greenhouse study the MSN treatment had greater impacts on chlorophyll content, although the CTS-MSN still exerted benefit. This difference is likely the result of inherent differences between greenhouse and field studies. In the greenhouse study, MSNs aid plant growth and suppress Fusarium, showing immediate effects over the shorter term, under less than ideal growth conditions; however, in the long-term and more amenable field conditions, CTS-MSNs have more of an impact. Although the exact mechanisms for this difference remain unknown, the rate of transformation and dissolution of the particles (shown in Figure 2 with CTS-MSNs dissolving slower than MSNs) under the different conditions could clearly be relevant. Additionally, chitosan has been shown to enhance disease resistance by triggering a signaling cascade within plants, thereby boosting their natural defense mechanisms. Chitosan also possesses antifungal properties that can offer protection against pathogens. Collectively, all of these factors could drive the greater impacts of CTS-MSNs under field conditions. Importantly, it should be noted that in both studies, the nanoscale materials still outperformed both conventional treatments.

There were few changes in biomasses across the treatments, indicating that disease pressure was very low in this field study (Figure 7). However, for infected plants, CTS-MSN treatment resulted in increased shoot and soybean pod masses compared to the other treatments, although the effect precluded statistical significance. Notably, the chitosan and silicic acid treatments showed a reduction in the biomasses of infected plants, although the decreases were not of statistical significance. This suggests that a combination of chitosan and silica at the nanoscale is necessary for plant benefit. Larger differences are expected in a field study with higher disease pressure. However, these results agree with previous work by Kumaraswamy et al. where a

chitosan-silicon nanofertilizer increased chlorophyll content and biomass in maize (*Zea mays* L.), enhancing crop health and yield with both a seed and foliar application.⁵⁰ Buchman et al. also

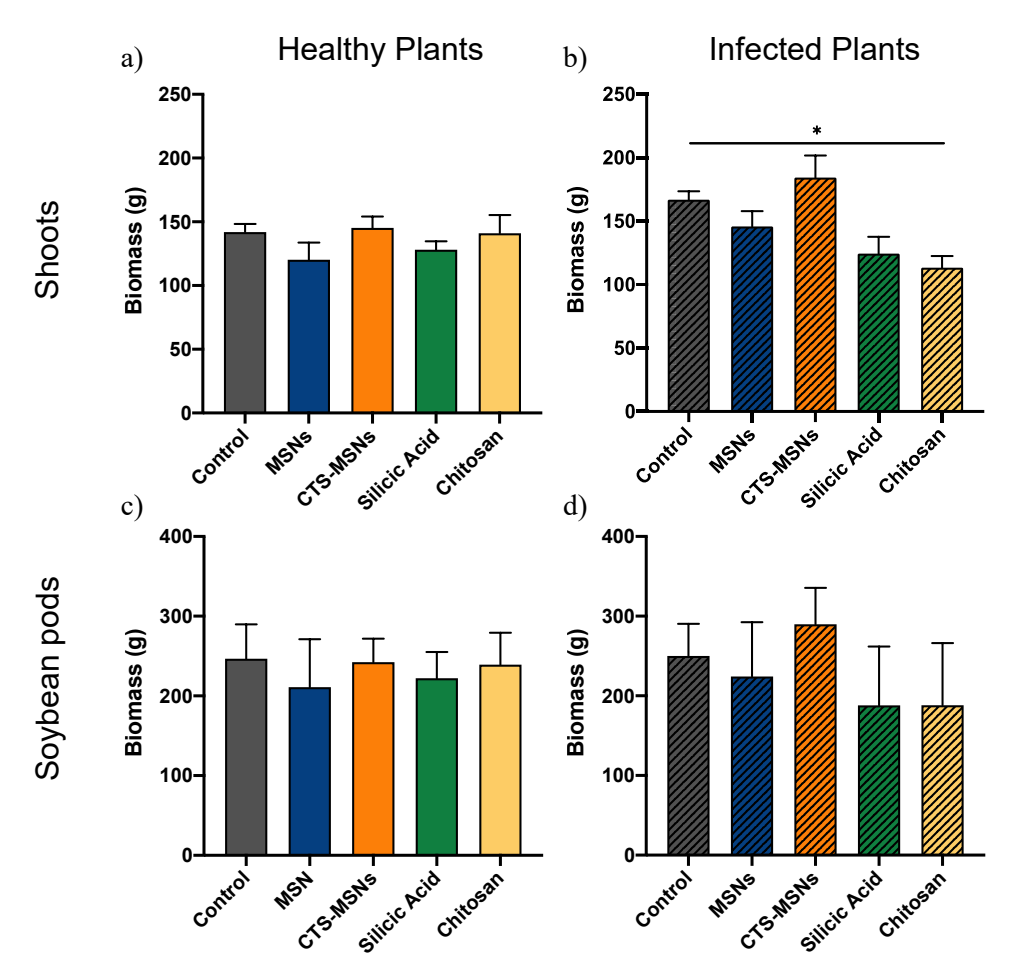


Figure 7. Field data for fresh weight for the shoots of (a) healthy plants and (b) *Fusarium*-infected plants as well as the soybean pods of (c) healthy plants and (d) *Fusarium*-infected plants. The error bars represent the standard error of five replicate plants. A one-way ANOVA with Dunnett's multiple comparisons was used to evaluate the statistical significance. *p < 0.05

reported that CTS-MSNs significantly reduced disease severity in watermelon (*Citrullus lanatus*) and increased the fruit yield in healthy plants by 70% compared to the control group. Furthermore, several previous studies that have investigated other NPs on a range of plants have correlated reduced disease with increased biomass, ^{16, 17} aligning well with the trends reported herein.

Si Content in Soybeans Post Harvest. The content of Si in shoots, roots, and soybean pods are shown in Figure 8. In shoots (Figure 8a,b), MSNs and CTS-MSNs significantly increased Si

content compared to the controls under the healthy condition by 105% and 88%, respectively. For the infected plants, only silicic acid increased Si content compared with the control (by 65%); no statistically significant differences were found for the nanoscale Si-based treatments. In roots (Figure 8c, d), both MSNs and silicic acid significantly increased Si content by over 200%; CTS-MSNs increased root Si content by 68%, although high replicate variability precluded statistical significance. For the infected plants, no statistically significant changes were observed as a function of treatment; however, the Si content was nominally the greatest in the MSN and CTS-MSN treatments. Notably, the pod Si content (Figure 8e,f) was significantly increased by MSNs by 147% and 71% for healthy and infected plants, respectively. None of the other treatments enhanced the pod Si content. While not statistically significant, the CTS-MSNs treatment resulted in greater Si content in all plant tissues compared to controls, which likely contributed to the greater biomasses and enhanced plant health observed in this field study. Xu et al. previously reported that root exposure to Si-based nanoparticles significantly increased the Si content within shoots and edible tissues of cherry radish (Raphanus sativus L.), resulting in enhance crop health and yield.⁵¹ This effect has also been reported for rice (*Orzya sativa* L.)⁵² and cucumber (*Cucumis* sativus L.).⁵³ Interestingly, significant increases in Si content were observed with MSN treatments, although no corresponding increases were evident in the plant health measurements. The reason for the lack of correlation in these effects is not known, although the fact that seed or foliar treatment of seedlings resulted in increased Si content at field harvest weeks later is certainly of interest. A time-dependent molecular study (gene expression, protein, or metabolite profiling) is needed to elucidate the underlying mechanism of actions and will be the subject of future work.

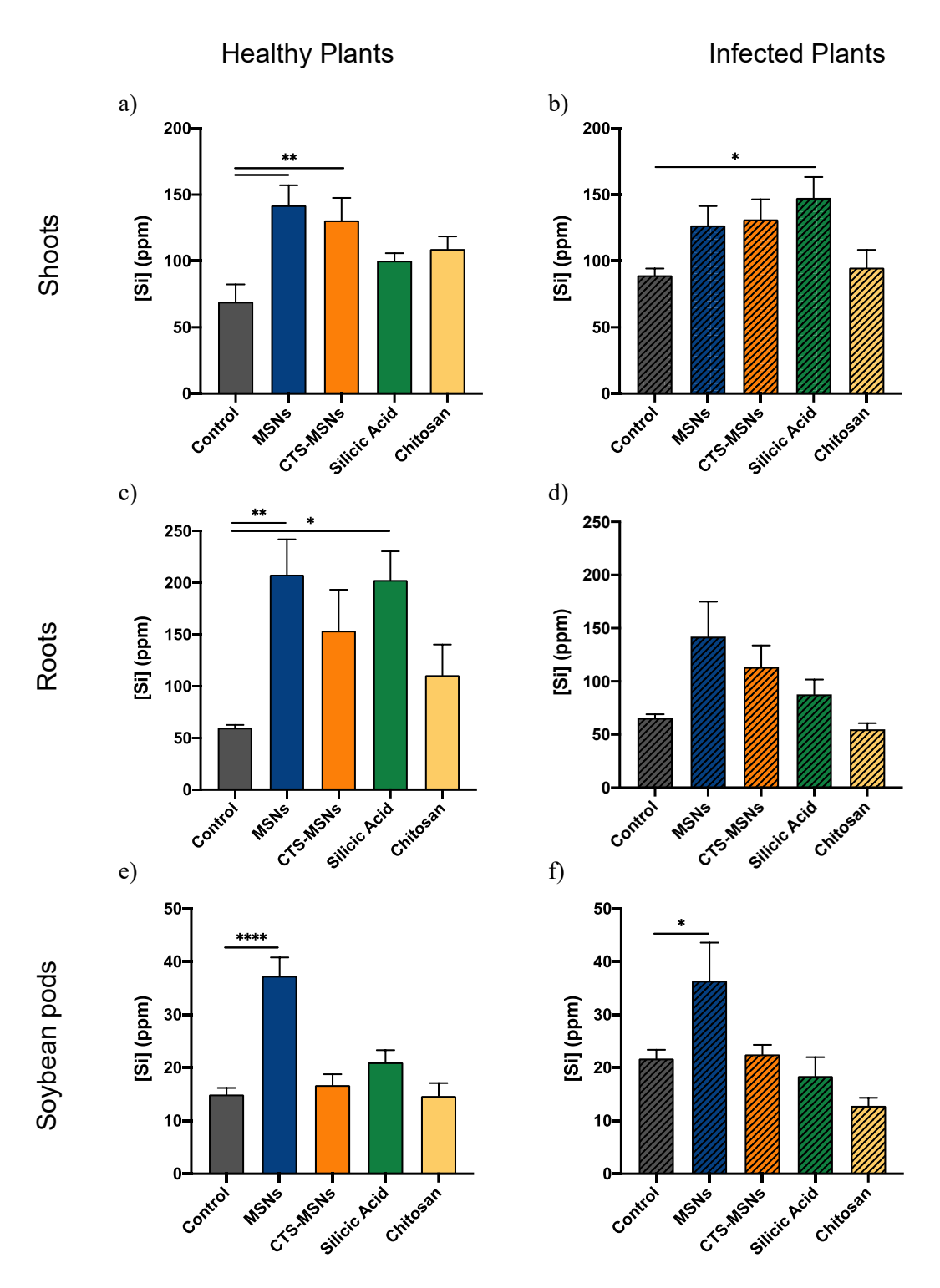


Figure 8. ICP-OES for shoots of (a) healthy plants and (b) *Fusarium*-infected plants; roots of (c) healthy plants and (d) *Fusarium*-infected plants; soybean pods for (e) healthy plants and (f) *Fusarium*-infected plants from the field study. The error bars represent the standard error of five replicate plants. A one-way ANOVA with Dunnett's multiple comparisons was used to evaluate statistical significance. *p < 0.05, **p < 0.01, ****p < 0.001

Macro-/micronutrient Accumulation. The nutritional profile of soybean pods collected from plants grown under healthy or diseased conditions in the field was determined (Figure 9). In healthy pods, MSNs significantly increased the accumulation of B, K, Mn, and Mg by 30%, 43%, 33%, and 68%, respectively, as compared to untreated controls (Figure 9 a-d). Notably, the silicic acid and chitosan treatment exerted no positive impacts on pod nutritional profile. Although CTS-MSNs led to slight increases in these elements, the changes were not statistically significant. The one exception to this is Zn; CTS-MSNs exposure did significantly enhance pod Zn accumulation by 23% compared to controls, while MSNs had no such impact. However, on the whole the micronutrient profile of the pods aligns well with the Si content (Figure 7); MSNs led to the most significant enrichment of these nutrients. For completeness, other macro-/micronutrients that were analyzed, but showed no statistical differences in healthy pods include, Al, Ca, Cu, Fe, P, S, and Ti. Interestingly, under the stress of pathogen pressure, the micronutrient content of the pods was largely unaffected by nanoscale silica treatment (Figure S5).

Micronutrients such as boron (B), zinc (Zn), and manganese (Mn) are not only vital for plant growth and serve pivotal roles in cell wall construction, sugar transport, and antioxidant defense, but are also critical components of the human diet. In fact, although chronic hunger and food insecurity affects over 800 million people globally, micronutrient deficiencies or hidden hunger afflicts 2 billion persons on a daily basis. ⁵⁴ Zn, in particular, holds significant importance; many agricultural soils globally suffer from Zn deficiency, which has directly led to significant human health impacts. Any sustainable strategy to promote micronutrient biofortification during routine crop cultivation is of tremendous interest. In addition, potassium (K) and magnesium (Mg) are essential micronutrients needed by plants in relatively large quantities for growth and daily functions, including chlorophyll synthesis, enzyme activation, and disease resistance. Notably,

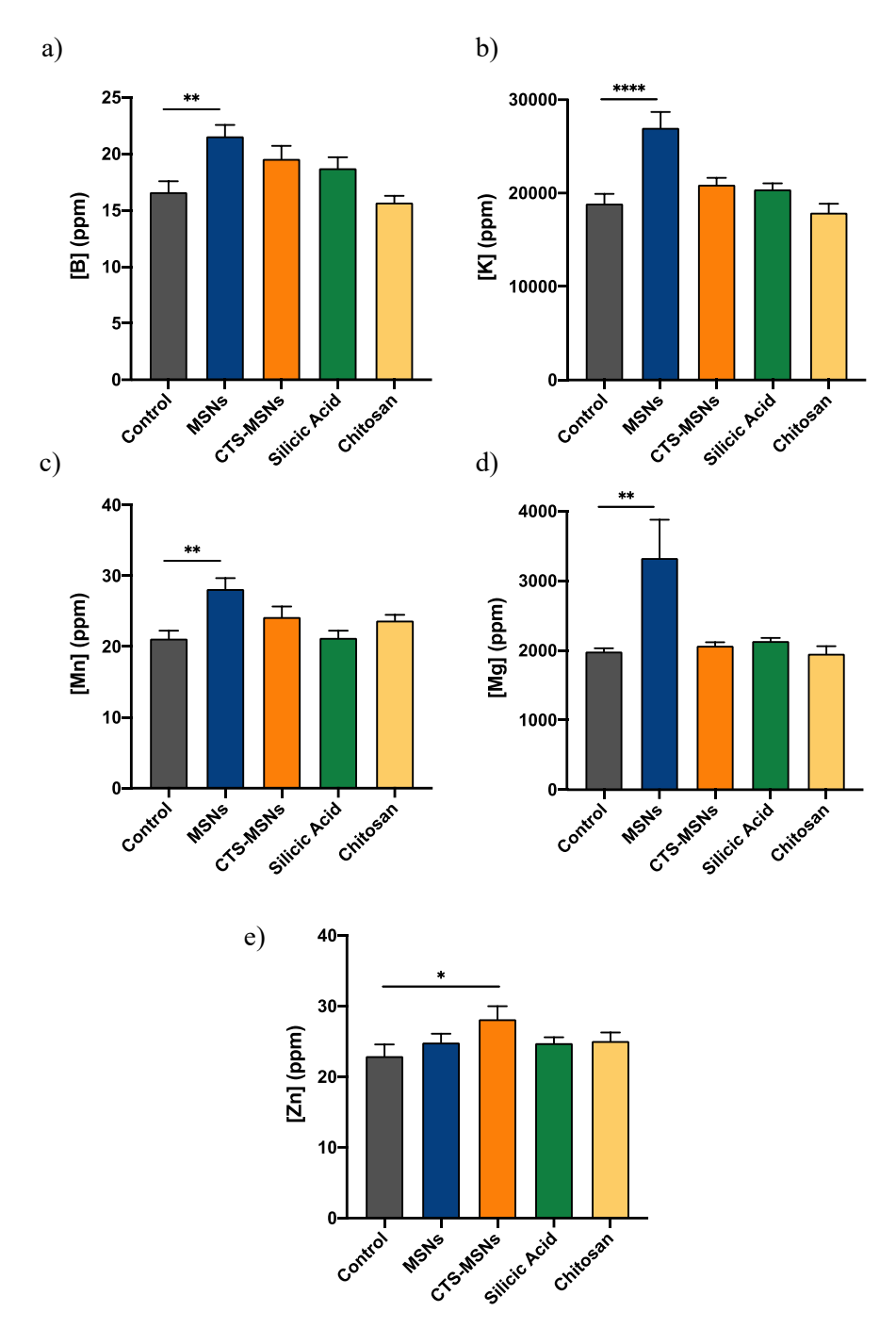


Figure 9. Concentration of (a) B, (b) K, (c) Mn, (d) Mg, and (e) Zn in the soybean pods of healthy plants as determined by ICP-OES. The error bars represent the standard error of five replicate plants. A one-way ANOVA with Dunnett's multiple comparisons was used to evaluate statistical significance. *p < 0.05, **p < 0.01, ****p < 0.0001

similar findings of nano-enabled nutrient increases have been previously reported. Although the mechanisms of action remain unknown, nanoscale silica is known to enhance the activity of a

number of enzyme systems, alter root morphology and function, and impact the rhizosphere microbial community, all of which could impact nutrient accumulation form soil. ^{15,17} For instance, Dimkpa et al. discovered that chitosan-coated tripolyphosphate (TPP) nanoscale material increased sulfur (S) element accumulation in wheat grain, while uncoated TPP showed no significant changes compared to conventional fertilizer control. ⁵⁵ Similarly, Trujillo-Reyes et al. found that bare CeO₂ nanoparticles enhanced manganese (Mn) content in radish seedlings, whereas citric acid-coated CeO₂ did not. ⁵⁶ These discoveries underscore the substantial knowledge gap concerning the impact nanomaterial surface chemistry properties have on the interplay between plants and nanoparticles. However, the findings provide an important foundational perspective on the potential for nano-enabled biofortification of food crops.

Overall, these results show the potential of MSNs and CTS-MSNs to suppress disease associated with common and problematic fungal pathogens of soybean (*Glycine max*), while simultaneously promoting plant growth and nutritional status, providing a sustainable solution in support of nano-enabled agriculture. Specifically, the greenhouse study compared the efficacy of foliar treatment to a vacuum infiltration seed treatment on healthy and *Fusarium*-infected soybean plants. A single seed infiltration with MSNs resulted in a reduction of disease severity by 30% which correlated well with significantly greater concentrations of *in planta* Si being incorporated during the infiltration process. Additionally, MSN treatment increased the chlorophyll content by 12% in both healthy and infected plants. Importantly, the conventional treatments conveyed no benefit, highlighting the importance of the particle size or transformation products of the nanoscale materials. Based on greenhouse results, a seed treatment was also evaluated under field conditions. In the field, CTS-MSNs reduced disease severity by 15% and significantly increased chlorophyll content by 32%. Nanoscale silica treatments also significantly increased the micronutrient (Zn,

Mn, Mg, K, and B) content of soybean pods by 23-68%, revealing their potential for nano-enabled

biofortification of soybeans. Together, these studies show that MSNs and CTS-MSNs increase

plant performance under disease pressure in the complete absence of conventional fungicides.

Future work will investigate the time-dependent mechanisms by which MSNs and CTS-

MSNs suppress disease damage, increase chlorophyll content, and promote soybean biomass under

a range of treatment regimes. In addition, future field studies, for both these nanomaterials and

others, should be performed at multiple locations to provide an understanding on the impacts of

soil type and environmental factors on MSN and CTS-MSN performance. Furthermore, a complete

life cycle assessment is needed to accurately quantify the benefits of MSN and CTS-MSN

treatment.

Supporting Information.

The Supporting Information includes representative thermograms of MSNs and CTS-MSNs, and

greenhouse and vacuum infiltration ICP-OES data. (PDF)

AUTHOR INFORMATION

Corresponding Author

*Corresponding author: chaynes@umn.edu

ORCID

Tana L. O'Keefe: 0000-0001-9480-4779

Chaoyi Deng: 0000-0002-7298-3216

Yi Wang: 0000-0002-2891-0386

Andres Torres-Gómez: 0000-0002-3121-527X

Beza S. Tuga: 0000-0002-1518-6050

Cheng-Hsin Huang: 0009-0004-2523-445X

Wilanyi R. Alverez Reyes: 0000-0001-8502-819X

28

Jason C. White: 0000-0001-5001-8143

Christy L. Haynes: 0000-0002-5420-5867

Present Address

Andres Torres-Gómez: Center for Research and Advanced Studies of the National Polytechnic

Institute (CINVESTAV) Saltillo Unit; Ramos Arizpe Coahuila, Mexico.

Author Contributions

† These authors contributed equally to this work.

‡ These authors contributed equally to this work.

Notes

The authors declare no competing financial interests.

ACKNOWLEDGMENTS

This work was supported by the National Science Foundation under Grant No. CHE-2001611,

the NSF Center for Sustainable Nanotechnology. The CSN is part of the Centers for Chemical

Innovation Program. The TEM imaging in this study was carried out in the Characterization

Facility, University of Minnesota, which receives partial support from the National Science

Foundation through the MRSEC program (Award number DMR-2011401). S.M. acknowledges

support from the Louis Stokes North Star STEM Alliance and the Louis Stokes Alliance for

Minority Participation (NSF grant #1712629). B.S.T acknowledges support from the University

of Minnesota's Doctoral Dissertation Fellowship. W.A.R. acknowledges support from the NIH

Chemical Biology Interface Training Grant: NIH 5T32GM132029-5. The authors acknowledge

Dr. Marc A. Hillmyer for the use of his thermogravimetric analyzer.

29

References

- 1. FAO, The State of Food and Agriculture Leveraging Food Systems for Inclusive Rural Transformation. **2017**.
- 2. FAO, Agricultural production statistics (2000-2021). 2022.
- 3. Savary, S.; Ficke, A.; Aubertot, J.-N.; Hollier, C., Crop losses due to diseases and their implications for global food production losses and food security. *Food Security* **2012**, *4* (4), 519-537.
- 4. Wang, H.; Xiao, M.; Kong, F.; Chen, S.; Dou, H. T.; Sorrell, T.; Li, R. Y.; Xu, Y. C., Accurate and practical identification of 20 Fusarium species by seven-locus sequence analysis and reverse line blot hybridization, and an in vitro antifungal susceptibility study. *J Clin Microbiol* **2011**, *49* (5), 1890-8.
- 5. Brar, H. K.; Swaminathan, W.; Bhattacharyya, M.K., The *Fusarium virguliforme* Toxin FvTox1 Causes Foliar Sudden Death Syndrome-Like Symptoms in Soybeans. *Molecular Plant-Microbe Interactions* **2011**, *24* (10), 1179-1188.
- 6. Pudake, R. N.; Swaminathan, S.; Sahu, B. B.; Leandro, L. F.; Bhattacharyya, M. K., Investigation of the Fusarium virguliforme fvtox1 mutants revealed that the FvTox1 toxin is involved in foliar sudden death syndrome development in soybean. *Curr Genet* **2013**, *59* (3), 107-17.
- 7. Allen, T. W.; Bradley, C. A.; Sisson, A. J.; Byamukama, E.; Chilvers, M. I.; Coker, C. M.; Collins, A. A.; Damicone, J. P.; Dorrance, A. E.; Dufault, N. S.; Esker, P. D.; Faske, T. R.; Giesler, L. J.; Grybauskas, A. P.; Hershman, D. E.; Hollier, C. A.; Isakeit, T.; Jardine, D. J.; Kelly, H. M.; Kemerait, R. C.; Kleczewski, N. M.; Koenning, S. R.; Kurle, J. E.; Malvick, D. K.; Markell, S. G.; Mehl, H. L.; Mueller, D. S.; Mueller, J. D.; Mulrooney, R. P.; Nelson, B. D.; Newman, M. A.; Osborne, L.; Overstreet, C.; Padgett, G. B.; Phipps, P. M.; Price, P. P.; Sikora, E. J.; Smith, D. L.; Spurlock, T. N.; Tande, C. A.; Tenuta, A. U.; Wise, K. A.; Wrather, J. A., Soybean Yield Loss Estimates Due to Diseases in the United States and Ontario, Canada, from 2010 to 2014. *Plant Health Progress* 2017, 18 (1), 19-27.
- 8. Bandara, A. Y.; Weerasooriya, D. K.; Bradley, C. A.; Allen, T. W.; Esker, P. D., Dissecting the economic impact of soybean diseases in the United States over two decades. *PLoS One* **2020**, *15* (4), e0231141.

- 9. Kandel, Y. R.; Lawson, M. N.; Brown, M. T.; Chilvers, M. I.; Kleczewski, N. M.; Telenko, D. E. P.; Tenuta, A. U.; Smith, D. L.; Mueller, D. S., Field and Greenhouse Assessment of Seed Treatment Fungicides for Management of Sudden Death Syndrome and Yield Response of Soybean. *Plant Dis* **2023**, *107* (4), 1131-1138.
- 10. Hartman, G. L.; Chang, H. X.; Leandro, L. F., Research advances and management of soybean sudden death syndrome. *Crop Protection* **2015**, *73*, 60-66.
- 11. Chawla, S. B., C.R.; Slaminko, T.L.; Hobbs, H.A.; Hartman, G.L., A Public Program to Evaluate Commercial Soybean Cultivars for Pathogen and Pest Resistance. *Plant Disease* **2013**, *97* (5), 568-578.
- 12. Lin, F.; Chhapekar, S. S.; Vieira, C. C.; Da Silva, M. P.; Rojas, A.; Lee, D.; Liu, N.; Pardo, E. M.; Lee, Y. C.; Dong, Z.; Pinheiro, J. B.; Ploper, L. D.; Rupe, J.; Chen, P.; Wang, D.; Nguyen, H. T., Breeding for disease resistance in soybean: a global perspective. *Theor Appl Genet* **2022**, *135* (11), 3773-3872.
- 13. Vick, C. M.; Chong, S.K.; Bond, J.P.; Russin, J.S., Response of Soybean Sudden Death Syndrome to Subsoil Tillage. *Plant Disease* **2003**, *87* (6), 629-632.
- 14. Leandro, L. L., M.; Chase, C., Crop diversification: Impact on weeds, soybean sudden death syndrome and crop producitivity. In *Proceedings of he 24th Annual Integrated Crop Management Conference*, 2012.
- 15. Buchman, J. T.; Elmer, W. H.; Ma, C.; Landy, K. M.; White, J. C.; Haynes, C. L., Chitosan-Coated Mesoporous Silica Nanoparticle Treatment of Citrullus lanatus (Watermelon): Enhanced Fungal Disease Suppression and Modulated Expression of Stress-Related Genes. *ACS Sustainable Chemistry & Engineering* **2019**.
- 16. Borgatta, J.; Ma, C.; Hudson-Smith, N.; Elmer, W.; Plaza Pérez, C. D.; De La Torre-Roche, R.; Zuverza-Mena, N.; Haynes, C. L.; White, J. C.; Hamers, R. J., Copper Based Nanomaterials Suppress Root Fungal Disease in Watermelon (Citrullus lanatus): Role of Particle Morphology, Composition and Dissolution Behavior. *ACS Sustainable Chemistry & Engineering* **2018**, *6* (11), 14847-14856.
- 17. Kang, H.; Elmer, W.; Shen, Y.; Zuverza-Mena, N.; Ma, C.; Botella, P.; White, J. C.; Haynes, C. L., Silica Nanoparticle Dissolution Rate Controls the Suppression of Fusarium Wilt of Watermelon (Citrullus lanatus). *Environmental Science & Technology* **2021**.

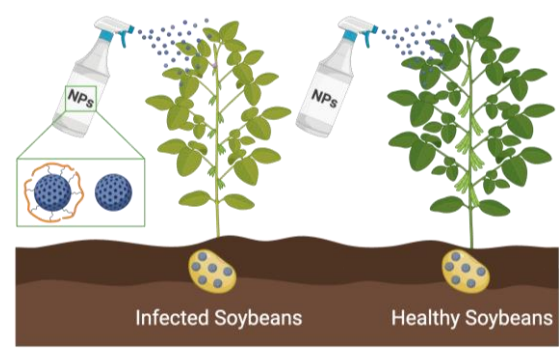
- 18. Ma, C.; Borgatta, J.; De La Torre-Roche, R.; Zuverza-Mena, N.; White, J. C.; Hamers, R. J.; Elmer, W. H., Time-Dependent Transcriptional Response of Tomato (Solanum lycopersicum L.) to Cu Nanoparticle Exposure upon Infection with Fusarium oxysporum f. sp. lycopersici. *ACS Sustainable Chemistry & Engineering* **2019**, *7* (11), 10064-10074.
- 19. Adisa, I. O.; Reddy Pullagurala, V. L.; Rawat, S.; Hernandez-Viezcas, J. A.; Dimkpa, C. O.; Elmer, W. H.; White, J. C.; Peralta-Videa, J. R.; Gardea-Torresdey, J. L., Role of Cerium Compounds in Fusarium Wilt Suppression and Growth Enhancement in Tomato (Solanum lycopersicum). *J Agric Food Chem* **2018**, *66* (24), 5959-5970.
- 20. Ahmed, A. I. S.; Yadav, D.R.; Lee, Y., Applications of Nickel Nanoparticles for Control of Fusarium Wilt on Lettuce and Tomato. *International Journal of Innovative Research in Science, Engineering and Technology* **2016**, *5* (5), 7378-7385.
- 21. Currie, H. A.; Perry, C. C., Silica in plants: biological, biochemical and chemical studies. *Ann Bot* **2007**, *100* (7), 1383-9.
- 22. Mathur, P.; Roy, S., Nanosilica facilitates silica uptake, growth and stress tolerance in plants. *Plant Physiol Biochem* **2020**, *157*, 114-127.
- 23. Fauteux, F.; Remus-Borel, W.; Menzies, J. G.; Belanger, R. R., Silicon and plant disease resistance against pathogenic fungi. *FEMS Microbiol Lett* **2005**, *249* (1), 1-6.
- 24. Li, W.; Zhou, H.; Zhang, X.; Li, Z.; Zou, Z.; Shen, Y.; Wang, G., Oxidation-Resistant Silicon Nanosystem for Intelligent Controlled Ferrous Foliar Delivery to Crops. *ACS Nano* **2023**, *17* (15), 15199-15215.
- 25. Zhao, P.; Yuan, W.; Xu, C.; Li, F.; Cao, L.; Huang, Q., Enhancement of Spirotetramat Transfer in Cucumber Plant Using Mesoporous Silica Nanoparticles as Carriers. *J Agric Food Chem* **2018**, *66* (44), 11592-11600.
- 26. Sun, D.; Hussain, H. I.; Yi, Z.; Siegele, R.; Cresswell, T.; Kong, L.; Cahill, D. M., Uptake and cellular distribution, in four plant species, of fluorescently labeled mesoporous silica nanoparticles. *Plant Cell Rep* **2014**, *33* (8), 1389-402.
- 27. Wang, J.; Li, R.; Zhao, Z.; Zhu, M.; Wang, Y., Bioactivity, Uptake, and Distribution of Prothioconazole Loaded on Fluorescent Double-Hollow Shelled Mesoporous Silica in Soybean Plants. *J Agric Food Chem* **2023**, *71* (11), 4521-4535.
- 28. El Hadrami, A.; Adam, L. R.; El Hadrami, I.; Daayf, F., Chitosan in plant protection. *Mar Drugs* **2010**, *8* (4), 968-87.

- 29. Chandra, S.; Chakraborty, N.; Dasgupta, A.; Sarkar, J.; Panda, K.; Acharya, K., Chitosan nanoparticles: A positive modulator of innate immune responses in plants. *Sci Rep* **2015**, *5*, 15195. 30. Saharan, V.; Mehrotra, A.; Khatik, R.; Rawal, P.; Sharma, S. S.; Pal, A., Synthesis of chitosan based nanoparticles and their in vitro evaluation against phytopathogenic fungi. *Int J Biol Macromol* **2013**, *62*, 677-83.
- 31. Xing, K.; Zhu, X.; Peng, X.; Qin, S., Chitosan antimicrobial and eliciting properties for pest control in agriculture: a review. *Agronomy for Sustainable Development* **2014**, *35* (2), 569-588.
- 32. Narasimhamurthy, K.; Udayashanka, A.C.; De Britto, S.; Lavanya, S.N.; Abdelrahman, M.; Soumya, K.; Shekar Shetty, H.; Srinivas, C.; Jogaiah, S., Chitosan and chitosan-dervied nanoparticles modulate enhanced immune response in tomato against bacterial wilt disease. *International Journal of Biological Macromolecules* **2022**, *220*, 223-237.
- 33. Sathiyabama, M.; Gaandhi, M.; Indhumanthi, M., Suppression of dry root rot diseased caused by *Rhizoctonia bataticola* (Taub.) Butler in chickpea plants by application of thiamine loaded chitosan nanoparticles. *Microbial Pathogenesis* **2022**, *173*, 105893.
- 34. Nguyen, N. T.; Nguyen, D. H.; Pham, D. D.; Dang, V. P.; Nguyen, Q. H.; Hoang, D. Q., New oligochitosan-nanosilica hybrid materials: preparation and application on chili plants for resistance to anthracnose disease and growth enhancement. *Polymer Journal* **2017**, *49* (12), 861-869.
- 35. Saberi Riseh, R.; Vatankhah, M.; Hassanisaadi, M.; Kennedy, J. F., Chitosan/silica: A hybrid formulation to mitigate phytopathogens. *Int J Biol Macromol* **2023**, *239*, 124192.
- 36. Lin, Y. S.; Abadeer, N.; Hurley, K. R.; Haynes, C. L., Ultrastable, redispersible, small, and highly organomodified mesoporous silica nanotherapeutics. *J Am Chem Soc* **2011**, *133* (50), 20444-57.
- 37. Chen, F.; Zhu, Y., Chitosan enclosed mesoporous silica nanoparticles as drug nano-carriers: Sensitive response to the narrow pH range. *Microporous and Mesoporous Materials* **2012**, *150*, 83-89.
- 38. Coradin, T.; Eglin, D.; Livage, J., The silicomolybdic acid spectrophotometric method and its application to silicate/biopolymer interaction studies. *Spectroscopy* **2004**, *18*, 567-576.
- 39. Wang, Y.; Deng, C.; Shen, Y.; Borgatta, J.; Dimkpa, C. O.; Xing, B.; Dhankher, O. P.; Wang, Z.; White, J. C.; Elmer, W. H., Surface Coated Sulfur Nanoparticles Suppress Fusarium

- Disease in Field Grown Tomato: Increased Yield and Nutrient Biofortification. *J Agric Food Chem* **2022,** 70 (45), 14377-14385.
- 40. Deng, C.; Protter, C. R.; Wang, Y.; Borgatta, J.; Zhou, J.; Wang, P.; Goyal, V.; Brown, H.
- J.; Rodriguez-Otero, K.; Dimkpa, C. O.; Hernandez, R.; Hamers, R. J.; White, J. C.; Elmer, W.
- H., Nanoscale CuO charge and morphology control Fusarium suppression and nutrient biofortification in field-grown tomato and watermelon. *Sci Total Environ* **2023**, *905*, 167799.
- 41. Jeger, M. J.; Veiljanen-Rollinson., S.L.H., The use of the area under the disease-progress curve (AUDPC) to asses quantitative disease resistance in crop cultivars. *Theoretical and Applied Genetics* **2001**, *102*, 32-40.
- 42. Sen Karaman, D.; Sarwar, S.; Desai, D.; Bjork, E. M.; Oden, M.; Chakrabarti, P.; Rosenholm, J. M.; Chakraborti, S., Shape engineering boosts antibacterial activity of chitosan coated mesoporous silica nanoparticle doped with silver: a mechanistic investigation. *J Mater Chem B* **2016**, *4* (19), 3292-3304.
- 43. El-Shetehy, M.; Moradi, A.; Maceroni, M.; Reinhardt, D.; Petri-Fink, A.; Rothen-Rutishauser, B.; Mauch, F.; Schwab, F., Silica nanoparticles enhance disease resistance in Arabidopsis plants. *Nat Nanotechnol* **2020**.
- 44. Du, J.; Liu, B.; Zhao, T.; Xu, X.; Lin, H.; Ji, Y.; Li, Y.; Li, Z.; Lu, C.; Li, P.; Zhao, H.; Li, Y.; Yin, Z.; Ding, X., Silica nanoparticles protect rice against biotic and abiotic stresses. *J Nanobiotechnology* **2022**, *20* (1), 197.
- 45. Dimkpa, C. O.; Bindraban, P. S.; Fugice, J.; Agyin-Birikorang, S.; Singh, U.; Hellums, D., Composite micronutrient nanoparticles and salts decrease drought stress in soybean. *Agronomy for Sustainable Development* **2017**, *37* (1).
- 46. Dimkpa, C. O.; Singh, U.; Bindraban, P. S.; Adisa, I. O.; Elmer, W. H.; Gardea-Torresdey, J. L.; White, J. C., Addition-omission of zinc, copper, and boron nano and bulk oxide particles demonstrate element and size -specific response of soybean to micronutrients exposure. *Sci Total Environ* **2019**, *665*, 606-616.
- 47. Dimkpa, C. O.; Andrews, J.; Sanabria, J.; Bindraban, P. S.; Singh, U.; Elmer, W. H.; Gardea-Torresdey, J. L.; White, J. C., Interactive effects of drought, organic fertilizer, and zinc oxide nanoscale and bulk particles on wheat performance and grain nutrient accumulation. *Sci Total Environ* **2020**, *722*, 137808.

- 48. Li, Y.; Xi, K.; Liu, X.; Han, S.; Han, X.; Li, G.; Yang, L.; Ma, D.; Fang, Z.; Gong, S.; Yin, J.; Zhu, Y., Silica nanoparticles promote wheat growth by mediating hormones and sugar metabolism. *J Nanobiotechnology* **2023**, *21* (1), 2.
- 49. Sun, D.; Hussain, H. I.; Yi, Z.; Rookes, J. E.; Kong, L.; Cahill, D. M., Mesoporous silica nanoparticles enhance seedling growth and photosynthesis in wheat and lupin. *Chemosphere* **2016**, *152*, 81-91.
- 50. Kumaraswamy, R. V.; Saharan, V.; Kumari, S.; Chandra Choudhary, R.; Pal, A.; Sharma, S.
- S.; Rakshit, S.; Raliya, R.; Biswas, P., Chitosan-silicon nanofertilizer to enhance plant growth and yield in maize (Zea mays L.). *Plant Physiol Biochem* **2021**, *159*, 53-66.
- 51. Xu, X.; Guo, Y.; Hao, Y.; Cai, Z.; Cao, Y.; Fang, W.; Zhao, B.; Haynes, C. L.; White, J. C.; Ma, C., Nano-silicon fertiliser increases the yield and quality of cherry radish. *Modern Agriculture* **2023**, *1* (2), 152-165.
- 52. Kheyri, N.; Norouzi, H. A.; Mobasser, H. R.; Torabi, B., Effects of Silicon and Zinc Nanoparticles on Growth, Yield, and Biochemical Characteristics of Rice. *Agronomy Journal* **2019**, *111* (6), 3084-3090.
- 53. Li, S.; Liu, J.; Wang, Y.; Gao, Y.; Zhang, Z.; Xu, J.; Xing, G., Comparative physiological and metabolomic analyses revealed that foliar spraying with zinc oxide and silica nanoparticles modulates metabolite profiles in cucumber (Cucumis sativus L.). *Food and Energy Security* **2021**, *10* (1).
- 54. Kah, M.; Tufenkji, N.; White, J. C., Nano-enabled strategies to enhance crop nutrition and protection. *Nat Nanotechnol* **2019**, *14* (6), 532-540.
- 55. Dimkpa, C. O.; Deng, C.; Wang, Y.; Adisa, I. O.; Zhou, J.; White, J. C., Chitosan and Zinc Oxide Nanoparticle-Enhanced Tripolyphosphate Modulate Phosphorus Leaching in Soil. *ACS Agricultural Science & Technology* **2023**, *3* (6), 487-498.
- 56. Trujillo-Reyes, J.; Vilchis-Nestor, A. R.; Majumdar, S.; Peralta-Videa, J. R.; Gardea-Torresdey, J. L., Citric acid modifies surface properties of commercial CeO2 nanoparticles reducing their toxicity and cerium uptake in radish (Raphanus sativus) seedlings. *J Hazard Mater* **2013**, *263 Pt 2*, 677-84.

For Table of Contents Only



◆ Disease Suppression ◆ Chlorophyll Content ◆ Biomass ◆ Silicon Content

Synopsis: Application of mesoporous silica nanoparticles and chitosan-coated mesoporous silica nanoparticles increases micronutrient content of soybeans in healthy plants and suppresses disease in infected plants.